FewSense, Towards a Scalable and Cross-Domain Wi-Fi Sensing System Using Few-Shot Learning

Guolin Yin, Junqing Zhang, *Member, IEEE,* Guanxiong Shen, and Yingying Chen, *Fellow, IEEE*

Abstract—Wi-Fi sensing can classify human activities because each activity causes unique changes to the channel state information (CSI). Existing WiFi sensing suffers from limited scalability as the system needs to be retrained whenever new classes are added, which causes overheads of data collection and retraining. Cross-domain sensing may fail because the mapping between activities and CSI variations is destroyed when a different environment or user (domain) is involved. This paper proposed a few-shot learning-based WiFi sensing system, named FewSense, which can recognise novel classes in unseen domains with only a few samples. Specifically, a feature extractor was pre-trained offline using the source domain data. When the system was applied in the target domain, a few samples were used to fine-tune the feature extractor for domain adaptation. Inference was made by computing the cosine similarity. FewSense can further boost the classification accuracy by collaboratively fusing inference from multiple receivers. We evaluated the performance of FewSense using three public datasets, i.e., SignFi, Widar, and Wiar. The results show that FewSense with five-shot learning recognised novel classes in unseen domains with an accuracy of 93.9%, 96.5%, and 82.7% on the SignFi, Widar, and Wiar datasets, respectively. Our collaborative sensing model improved system performance by an average of 29.2%.

Index Terms—Wi-Fi sensing, few-shot learning, cross-domain sensing

1 Introduction

1.1 Overview

Wi-Fi sensing systems has recently received extensive research interests [1], [2]. Wi-Fi is widely available because it is built into many consumer electronics, including laptops, smartphones, tablets, wearable devices such as Fitbits, and smart home appliances, to name a few. Various interesting applications have been inspired, including large-scale movements such as human activity recognition [3]–[5], fall detection [6], [7], and gait recognition [8], [9], as well as small-scale movements such as gesture recognition [10], [11], sign language recognition [12], [13], and vital sign detection [14], [15]. These applications are very useful for our everyday life. For example, gesture recognition can be applied in human-computer interaction and smart home to enable smooth control of devices.

Wi-Fi transmissions experience line-of-sight propagation, reflection, refraction, and scattering, which are affected by the environment and the objects within it [16]. When a person performs an activity, e.g., walking or hand moving, the activity will cause unique changes to the radio propagation, which can be measured via the channel state information (CSI). Deep learning can be adopted to learn the unique mapping between the CSI patterns and activity types thanks to its effective feature extraction and classification capability [17]. A deep learning-based sensing approach involves two stages. In the training stage, a training dataset should be constructed and a deep learning model is trained offline. Specifically, when an activity is performed, the Wi-Fi signals will get perturbed. The receiver will estimate the CSI, whose variation is affected by the activity. Many CSI records are collected for each activity. The process is repeated for all the activities, and the training dataset is established. A deep learning model can then be trained offline, which only needs to be done once. During the testing stage, based on the captured CSI, the derived deep learning model will be utilised to infer the activity type.

Manuscript received xxx; revised xxx; accepted xxx. Date of publication xxx; date of current version xxx. The work was in part supported by National Key Research and Development Program of China under grant ID 2020YFE0200600. The review of this paper was coordinated by xxx. (Corresponding author: Junqing Zhang)

- *G. Yin, J. Zhang and G. Shen are with the Department of Electrical Engineering and Electronics, University of Liverpool, Liverpool, L69 3GJ, United Kingdom. (email: {Guolin.Yin, Junqing.Zhang, Guanxiong.Shen}@liverpool.ac.uk)*
- *Y. Chen is with Department of Electrical and Computer Engineering, Rutgers University, Piscataway, NJ 08854, US. (email: yingche@scarletmail.rutgers.edu)*

Color versions of one or more of the figures in this paper are available online at http://ieeexplore.ieee.org.
Digital Object Identifier xxx

1.2 Limitations of Existing Systems

Although the above deep learning-based sensing systems can recognise human activities with reasonable accuracy, there are still limitations that restrict practical applications.

1.2.1 *Limited Scalability*

A classic deep learning-based sensing system explores the uniqueness of the mapping between the CSI variations and activities. A common limitation of such systems is that they can only handle the same classes/activities as those used during the training process. Whenever a new class needs to be added to or an existing class needs to be removed from the well-trained model, the model should be retrained using data from the existing classes and the new classes. The retraining results in three types of overhead:

- The storage of the existing training data, which occupies hard disk space and requires extra maintenance.
- The collection of the new data is time-consuming and labour-intensive.
- The computational overhead for retraining is quite high when there is a large amount of data, which cannot be completed in real time.

However, adjusting, including adding and deleting, classes is common in practical applications, e.g., a new sign gesture may need to be enrolled. The lack of scalability in the current approach and design makes it difficult to be deployed in real-world scenarios.

1.2.2 Domain Shift

The radio signal experiences multipath propagation whose characteristics are determined by the environment and the sensing activity. The same activity performed in different environments will cause deviated CSI variations. In addition, the same activity performed by different users may also have deviated CSI variations because the users may perform the same activity in a slightly different way or their heights/body shapes are different. The parameters independent to the activity can be denoted as a domain [18], e.g., the environment and/or the user. Source and target domains refer to the domains of the training and testing stages, respectively.

When the source and target domains are different, domain shifting happens. The obtained CSI will differ, and the recognition performance will suffer as a result. However, it is very common to apply Wi-Fi sensing systems in different environments and/or for different users. Existing solutions can be classified into three categories, namely domain adversarial training-based [18], [19], transfer learning-based [20], and domain-independent feature-based [21] approaches. However, these approaches are subject to the following limitations:

- The domain adversarial training-based approach requires the training dataset to cover data from many domains, but there are numerous possible domains.
- The transfer learning-based approach needs extensive data from the target domain, which sometimes may not be possible. For example, the work in [20] requires 500 samples for transfer learning to achieve comparable accuracy with models trained without transfer learning. While the required samples for transfer learning are only one quarter of the amount required by training without transfer learning, transfer learning still requires quite extensive data, which may pose a big challenge.
- The domain-independent feature-based method relies on special knowledge to design unique features and may also need extra receivers, e.g., body-coordinate velocity profile (BVP) in [21]. In addition, it may suffer from high computational costs, which would make it impossible for practical use.

Hence, a lightweight cross-domain sensing approach is urgently required to reduce the overhead of collecting data from source or target domains as well as eliminate the constraints of extra hardware and computational resources.

1.3 Few-Shot Learning

Few-shot learning (FSL) has been widely investigated in computer vision for image classification [22]. A classic deep learning model aims to learn the unique features of each class and predict the label based on the feature mapping. In contrast, FSL is a meta-learning technique. Instead of learning unique features, it makes predictions based on the similarity of the feature sets. Specifically, a feature extractor will be pre-trained using the base set. Then, a support set will be constructed with a few pairs of data and labels. Finally, a query set contains data whose label is to be inferred. The prediction is made by comparing the similarity between the features of the support and query sets.

FSL has recently been applied to Wi-Fi sensing as well [23] to address the scalability and cross-domain issues. The support set can be flexibly adjusted because very few samples are required for each class, and no cumbersome training is needed. The performance of FSL relies on the generalisation capability of the feature extractor, which however requires an extensive base set. Hence, the work in [23] designed a virtual gesture generation algorithm to transform existing gestures into virtual gestures. The base set can thus be enriched, and the overhead of data collection can be mitigated. However, designing the virtual gesture generation algorithm requires sophisticated knowledge that cannot be extended to other tasks straightforwardly.

The FSL is also employed in [24] and [25] to tackle the cross-environment problem in WiFi sensing. The researchers in [24] presented a dual-path base network for classifying activities and a metric-based meta-learning framework to enhance the base network's adaptability. The researchers in [25] proposed using the Siamese network for few-shot learning, and a multiple kernel variant of maximum mean discrepancies (MK-MMD) was introduced for minimising the domain shift such that the network can achieve cross-domain recognition. Their networks can be transferred to different environments for the same set of classes. However, when new classes are introduced to the system, their network models must be retrained using samples from both the new classes and the current classes. Thus, the scalability of these works is limited.

1.4 Contributions

In light of the initial success of using FSL in designing the virtual gesture generation algorithm [23], in this work, we further employ FSL to address the scalability issue and domain shift challenge faced by many practical Wi-Fi sensing applications. We demonstrated that the feature extractor can be generalised to a totally different sensing task. Specifically, we exploited a public dataset as the base set, applied the trained feature extractor to a different dataset, and achieved good classification performance, which is a different approach from [23]. In other words, our work aims to eliminate the need to construct an individual base set for every sensing task.

We adopt metric-based FSL for designing a scalable and cross-domain Wi-Fi sensing system. A CNN backbone is revised from the classic AlexNet architecture as the feature extractor. We design a collaborative sensing scheme to leverage the spatial diversity gain enabled by multiple receivers. The proposed model is evaluated using three public datasets, i.e, SignFi [12], Widar 3.0 [21] and Wiar [26]. We study in-domain sensing, cross-domain sensing, and cross-dataset sensing. Our findings show that the proposed FSL-based sensing system outperforms state-of-the-art works in the literature. Our contributions are summarised as follows:

- We propose an FSL-based Wi-Fi sensing system, FewSense, which is capable of novel class recognition and cross-domain sensing. Specifically, the proposed system can achieve 76.3% cross-domain accuracy for 76 novel sign language gestures using only one labelled sample for each novel class from the target domain when all the data is from the SignFi dataset.
- FewSense can be fine-tuned to new sensing tasks using a few samples. When the feature extractor is trained on the SignFi dataset (sign language recognition), evaluation over the Widar (gesture recognition) and Wiar (human activity recognition) datasets can achieve an average accuracy of 96.5% and 82.7%, respectively, with five samples from each novel class.
- A collaborative sensing approach is proposed to leverage the spatial diversity gain when there are multiple receivers. We evaluated FewSense on the Widar dataset. The accuracy can be raised by an average of 29.2% when the number of receivers is extended to six with one sample from each class, and to a maximum of 100% with six receivers and five samples from each class.

The code[1] developed for this study is available online.

The rest of this paper is organised as follows. Section 2 shows the CSI model in the Wi-Fi sensing system and states the problem with the existing systems. Then we present the overview of our system design in Section 3. Section 4 introduces our metric-based FSL method in details and Section 5 presents our collaborative sensing model to enable multiple receivers to work collaboratively. The performance evaluation of FewSense is given in Section 6. We review innovative works of FSL and cross-domain Wi-Fi sensing works in Section 7. Finally, Section 8 concludes the paper.

2 Background and Motivation

2.1 Background

As shown in Fig. 1, when a signal is sent from a transmitter and captured by a receiver, it experiences various propagation paths in a multipath environment. Specifically, there are static paths, which may include line-of-sight (LOS) and signals reflected by static objects such as walls and furniture, e.g., tables. There are also dynamic paths, which are reflected and/or scattered by moving objects in the environment [27]. Taking gesture recognition as an example, the movement of the palm will lead to dynamic paths of signal propagation.

The channel model can be mathematically given as

$$h(\tau, t) = \sum_{s\in S} h(\tau_s, t)\delta(\tau - \tau_s) + \sum_{d\in D} h(\tau_d, t)\delta(\tau - \tau_d), \quad (1)$$

1. https://github.com/Guolin-Yin/FewSense

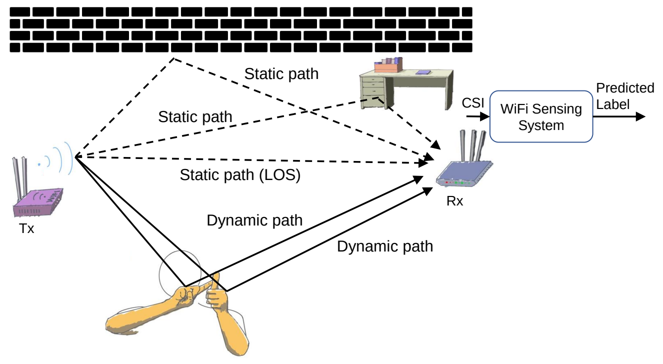

Fig. 1. Wi-Fi sensing model

where $h(\tau_s, t)$ and $h(\tau_d, t)$ are the channel attenuation of the static (grouped as $\{\mathcal{S}\}$) and dynamic paths (grouped as $\{\mathcal{D}\}$), respectively, and $\delta(\cdot)$ is the Dirac delta function. In the context of Wi-Fi sensing, orthogonal frequency-division multiplexing (OFDM) is the physical layer modulation used for IEEE 802.11a/g/n/ac/ax, which can obtain CSI in the frequency domain, given as

$$H(f, t) = \sum_{s\in S} h(\tau_s, t)e^{-j2\pi f\tau_s} + \sum_{d\in D} h(\tau_d, t)e^{-j2\pi f\tau_d}. \quad (2)$$

Objects and environments have a direct impact on CSI variations over time. Different gestures will have different moving patterns, which lead to unique CSI variations.

Deep learning can be adopted to reveal the relationship between the CSI variations and the corresponding gestures. By collecting a series of continuous packets when a gesture is performed, we can estimate and store records of CSI. During the training stage, the deep learning model can learn the specific patterns related to different gestures. Then, in the testing stage, the receiver will obtain a collection of CSI and infer the gestures based on the pre-trained deep learning model.

2.2 Motivation

Deep learning has been widely adopted for Wi-Fi sensing and has achieved excellent classification performance. Convolutional neural networks (CNN) [12], [28], and long-short term memory (LSTM) [25], [29] can learn and reveal complex feature patterns in a supervised learning manner. However, they are still subject to novel class recognition and cross-domain sensing.

2.2.1 *Limited Scalability/Novel Class Recognition*

In real-life applications, it is common to add new gestures to and/or remove existing ones from a gesture recognition system, which will result in changes in the number of classes (gestures). However, as already discussed, the classic deep learning techniques such as CNN and LSTM have limited scalability because they can only handle fixed-size classes once trained. Whenever new classes, e.g., unseen hand gestures, are added, the neural network model needs to be retrained with a massive number of training samples. Data collection and retraining overheads thus occur [23], [24], which are time-consuming and laborious.

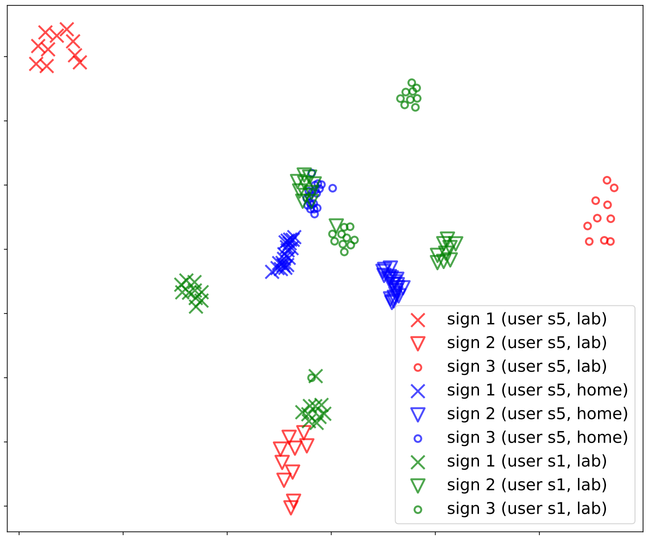

Fig. 2. t-SNE visualisation of the selected data from different domains: the same sign language from the same user but different environments, and different sign languages from the same environment but different users.

2.2.2 *Cross-Domain Sensing*

In order to achieve good classification performance, the training and test datasets should share the same distribution of data. Most existing works let the same user perform the gestures in the same environment [27], [30]. In other words, the static CSI part of (2) remains the same, but the dynamic part is uniquely caused by the gestures of the user. This is termed ”in-domain sensing,” where the domains refer to the environment and the user.

However, cross-domain sensing is actually more common in real-life deployments. The gestures will probably be performed by different users in different environments, i.e., cross-domain. The domain shift impacts the performance of Wi-Fi sensing systems for two reasons.

- When the environment changes, the static parts of (2) for training and testing are different, which results in different CSI patterns, i.e., varied data distributions.
- Different users may perform the same gesture in slightly different ways, which will also lead to different CSI dynamic parts of (2).

In order to illustrate the domain shift, we use sign languages from a public dataset SignFi [12] that will be introduced in Section 6.1.1. Specifically, we selected three sign gestures that are performed by two users at home and in a lab environment. Their distributions are visualised using t-SNE [31], which maps the CSI samples to a two-dimensional space. As shown in Fig. 2, the same sign performed in different environments or by different users has totally different distributions. Therefore, directly applying the neural network model trained on one domain to a new domain would not work.

3 System Design

3.1 System Overview

This paper employs metric-based FSL to address the above limitations. Our goal is to recognise novel classes in cross-domain scenarios, i.e., different environments and/or users, using only a few samples. Specifically, a three-stage approach is designed, namely feature extractor training, feature matrix generation, and classification, as shown in Fig. 3. Note that the same signal preprocessing algorithm is used for all three stages.

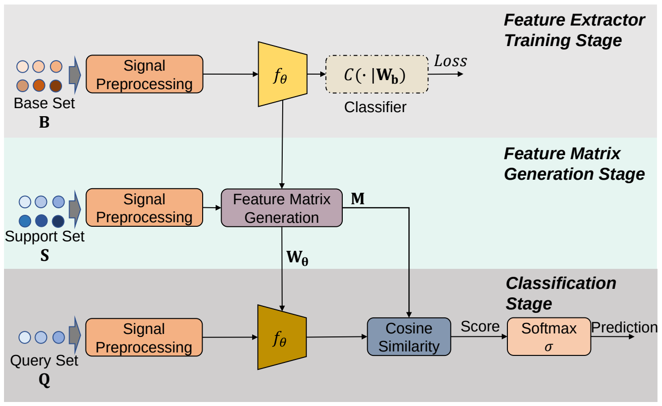

Fig. 3. The proposed metric-based FSL system for Wi-Fi sensing.

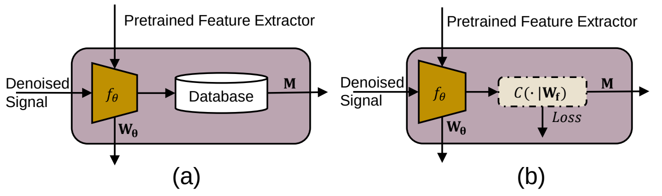

Fig. 4. The structure of two feature matrix generation methods.(a) Direct feature matrix generation. (b) Fine-tuned feature matrix generation.

3.2 Feature Extractor Training

We will first sample and preprocess raw CSI records and obtain CSI tensors $\mathbf{x}$, whose construction will be elaborated in Section 4.1. A base set, $\mathbf{B} = \left\{\left(\mathcal{X}^b, \mathcal{Y}^b\right)\right\}$, will be constructed by obtaining CSI tensors for different classes (e.g., sign gestures), where $\mathcal{X}^b = \left\{\mathbf{x}_1^b, \mathbf{x}_2^b, \cdots, \mathbf{x}_{\tilde{N}_b}^b\right\}$ are the CSI tensors and $\mathcal{Y}^b = \left\{y_1^b, y_2^b, \cdots, y_{\tilde{N}_b}^b\right\}$ are the corresponding labels. The number of instances in the base set is denoted as $\tilde{N}_b$, and $\tilde{N}_b = N_b \times K_b$, where N_b is the number of base classes and K_b is the number of samples per base class. The domain of the base set is referred to as the source domain, denoted as $\mathcal{D}_s$.

We use a standard supervised learning manner to train a feature extractor f_θ and a classifier $C\left(\cdot \mid \mathbf{W_b}\right)$, parameterised by $\mathbf{W}_\theta$ and $\mathbf{W_b}$, respectively. A large number of classes in the base set enables the feature extractor to learn unique latent features from base classes so that the distances between instances of the same class are closer while instances of different classes are further apart. Once the training is completed, the classifier will be removed to obtain the trained feature extractor. The training only needs to be done once.

3.3 Feature Matrix Generation

The data involved in this stage is called the support set, which is defined as $\mathbf{S} = \left\{\left(\mathcal{X}^s, \mathcal{Y}^s\right)\right\}$, where $\mathcal{X}^s =$

$\left\{\mathbf{x}_1^s, \mathbf{x}_2^s, \cdots, \mathbf{x}_{\tilde{N}_s}^s\right\}$ and $\mathcal{Y}^s = \left\{y_1^s, y_2^s, \cdots, y_{\tilde{N}_s}^s\right\}$ are the CSI tensors and labels, respectively. $\tilde{N}_s = N \times K$, where N is the number of novel classes, and K is the number of samples for each class. FSL is usually described as N-way K-shot classification. The classes in the support set have no overlap with the classes in the base set, i.e., $\mathcal{Y}^b \cap \mathcal{Y}^s = \emptyset$. Therefore, they are called novel classes. The domain of the support set is named as the target domain, denoted as $\mathcal{D}_t$. In practice the source domain and target domain are likely different, i.e., $\mathcal{D}_t \neq \mathcal{D}_s$, thus cross-domain sensing occurs.

We first collect K labelled shots (samples) for each novel class to construct the support set, which will be denoised by the preprocessing scheme. With samples from the support set, the pre-trained feature extractor f_θ will learn the latent feature representations of the novel classes, termed as the feature matrix in this paper. We propose two methods to generate it, i.e., direct feature matrix generation and fine-tuned feature matrix generation, as shown in Fig. 4.

- **Direct Feature Matrix Generation:** The feature extractor will extract the feature embedding directly from the support set. The feature embedding is stored in the database and output as the feature matrix.
- **Fine-tuned Feature Matrix Generation:** A new classifier will be introduced after the feature extractor. The weight matrix of the classifier and the feature extractor will be optimised using the samples in the support set. The adapted weight matrix will be the feature matrix.

3.4 Classification

The data involved in this stage is named as the query set $\mathbf{Q} = \{(\mathcal{X}^q, \mathcal{Y}^q)\}$, where $\mathcal{X}^q = \left\{\mathbf{x}_1^q, \mathbf{x}_2^q, \cdots, \mathbf{x}_{\tilde{N}_q}^q\right\}$ are the CSI tensors and $\mathcal{Y}^q = \left\{\mathbf{y}_1^q, \mathbf{y}_2^q, \cdots, \mathbf{y}_{\tilde{N}_q}^q\right\}$ represents the labels that to be inferred. Note that the support set and query set share the same label space and are performed in the same domain. Therefore, they have the same distribution.

The signal preprocessing scheme is used to remove the phase noise of the query set. The feature extractor, f_θ, is used to extract the latent features from the denoised query set. The final results are determined by computing the cosine similarity score between the latent features of the query set and the feature matrix generated from the previous stage.

4 Methodology

In this section, we first introduce the signal preprocessing algorithm that is used in all three stages of the proposed FSL-based system. We then elaborate on each of these three stages.

4.1 Signal Preprocessing

A Wi-Fi transmitter will continuously send packets that are captured by receivers within the communication range. The CSI can be estimated but will be impacted by sampling frequency offset (SFO), packet detection delay (PDD) and carrier frequency offset (CFO) [32], which can be given as

$$\widehat{H}(f, t) = e^{-j\phi(t)} H(f, t), \tag{3}$$

where $\phi(t)$ is the phase shift collectively caused by the above issues.

Most of the existing works only employ amplitude for sensing. The phase of CSI is more sensitive than the amplitude [6] and will be beneficial to the system performance. In this work, we leverage a linear transformation proposed in [33] to sanitise the CSI. According to the specific implementation of the Intel 5300 Wi-Fi network interface card (NIC) [34], the process can be given as

$$\angle\widetilde{H}(f_i, t) = \angle\widehat{H}(f_i, t) - k m_i - b, \tag{4}$$

where i is ranging from 1 to 30, f_i is the corresponding subcarrier frequency, m_i is the subcarrier index ranging from -28 to 28. IEEE 802.11 CSI tool reports one CSI every two subcarriers [34], and

$$k = \frac{\angle\widehat{H}(f_{30}, t) - \angle\widehat{H}(f_1, t)}{m_{30} - m_1}, \tag{5}$$

$$b = \frac{1}{30}\sum_{i=1}^{30} \angle\widehat{H}(f_i, t). \tag{6}$$

In this work, we concatenate the amplitude, $|\widehat{H}(f_i, t)|$, and the sanitised phase, $\angle\widetilde{H}(f_i, t)$. By combining the data from all the antennas, we finally construct a CSI tensor $\mathbf{x} \in \mathbb{R}^{U_s \times U_{ap} \times U_{ant}}$, where U_s is the number of sampling points, U_{ap} is the number of elements of amplitude plus phase, and the U_{ant} is the number of antenna pairs.

4.2 Feature Extractor Training Stage

The main purpose of the feature extractor training stage is to train a feature extractor that can extract discriminative features from input samples.

The structure of the feature extractor is shown in Fig. 5, which is revised from the classic AlexNet architecture [17]. An L_2-norm layer [35] is added before the classifier, which normalises the embedded latent feature vectors as follows:

$$f_\theta(\mathbf{x}) = \frac{f'_\theta(\mathbf{x})}{\|f'_\theta(\mathbf{x})\|_2}, \tag{7}$$

where $f'_\theta(\mathbf{x})$ is the output of the previous fully connected (FC) layer, and $\|\cdot\|_2$ denotes the L_2-norm operation. By adding an L_2-norm layer, the embedded features will be forced to lie on a hypersphere of a fixed radius [35]. Adopting L_2-norm layer will improve the system's converging speed and accuracy, because it forces the embedded features from the same class closer and moves the features from different classes further apart.

A classifier, $C(\cdot \mid \mathbf{W})$, consists of a fully connected layer with softmax activation function. In this stage, the classifier is parameterised by the weight matrix $\mathbf{W_b} \in \mathbb{R}^{n \times N_b}$, where n is the dimension of extracted features from the feature extractor. The classifier takes the normalised feature and then computes $(\mathbf{W_b})^\top f_\theta\left(\mathbf{x}_i^b\right)$, where $(\cdot)^\top$ denotes transpose operation. Finally, the prediction is made via the softmax function, mathematically given as

$$\sigma(\mathbf{v})_i = \frac{e^{v_i}}{\sum_{j=1}^{G} e^{v_j}}, \tag{8}$$

where $\mathbf{v}$ is the output of the fully connected layer, and G is the number of classes. Here, $\mathbf{v} = (\mathbf{W_b})^\top f_\theta\left(\mathbf{x}_i^b\right)$ and

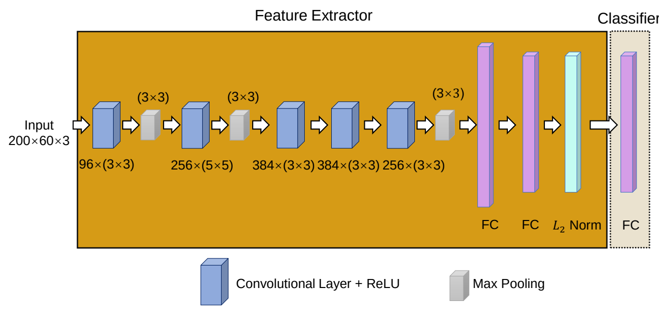

Fig. 5. The architecture of the feature extractor, modified AlexNet.

$G = N_b$. The output of the softmax function is a probability vector that represents confidence levels across different classes. The class with the highest probability is selected as the classification result.

We train the feature extractor using the samples from the base set, $\mathbf{B}$, in a supervised learning manner. The feature extractor will learn to extract distinct features from the CSI samples of different classes. It is crucial to carry out training with a sufficient number of base classes to enable the feature extractor to generalise to novel classes. Once the training is completed, the classifier is removed and the feature extractor is attained.

4.3 Feature Matrix Generation Stage

This stage aims to generate discriminative features for novel classes in the support set.

Firstly, one or a few samples from each novel class are obtained for the feature matrix generation. The corresponding CSI instances are added to the support set, $\mathbf{S}$. The signal preprocessing scheme will be performed on the support set data to get the input for the feature extractor. Depending on different deployment scenarios, two methods can be used in the feature matrix generation stage.

4.3.1 Direct Feature Matrix Generation

The feature extractor extracts the latent feature vectors from the denoised data. The support set embedding $\mathbf{F}_s \in \mathbb{R}^{n\times N}$ is obtained by computing the mean of the feature vector for each class, given as

$$\mathbf{F}_s = \left[\ f_\theta(\mathbf{x}_1^s), f_\theta(\mathbf{x}_2^s), \dots, f_\theta(\mathbf{x}_N^s)\ \right]. \tag{9}$$

The feature embeddings are saved in the database for future use. In this case, the output matrix $\mathbf{M}$ of this stage is the feature embedding, i.e., $\mathbf{M} = \mathbf{F}_s$, which will be fed into the next stage for classification. This method allows fast generation of distinctive feature matrix directly from the support set with little overhead.

4.3.2 Fine-Tuned Feature Matrix Generation

In some challenging scenarios, where the distributions of datasets or fundamental features may change dramatically, the feature extractor trained on the base set will fail in new sensing tasks. In order to adapt the feature extractor to new tasks, we propose a fine-tuned feature matrix generation scheme based on the fully labelled support set.

A classifier with the trainable weight matrix $\mathbf{W}_\mathrm{f} \in \mathbb{R}^{n\times N}$, initialised by the support set embedding $\mathbf{F}_s$, is added after the pre-trained feature extractor. The output of the softmax function is $\sigma((\mathbf{W}_\mathrm{f})^\top f_\theta(\mathbf{x}_i^s))$.

Fine-tuning is done by minimising the softmax loss based on the support set, which will update the parameters in the feature extractor f_θ and the weight matrix of the classifier $\mathbf{W}_\mathrm{f}$.

The output matrix of this method is the weight matrix of the classifier, i.e., $\mathbf{M} = \mathbf{W}_\mathrm{f}$. The fine-tuned feature extractor will be used in the next stage. The fine-tuned feature matrix generation method enhances the adaptivity of the model in new sensing domains or tasks.

4.4 Classification Stage

At this stage, each sample in the query set will be classified based on the cosine similarity score between the feature matrix and the extracted latent features of the query set.

An instance from the query set $\mathbf{Q}$ will be firstly processed by the preprocessing scheme. The feature extractor will extract an embedded feature vector $f_\theta(\mathbf{x}^q) \in \mathbb{R}^{n\times 1}$.

We compute the cosine similarity score of $f_\theta(\mathbf{x}^q)$ pairwisely with all the elements in $\mathbf{M}$ by

$$\mathbf{v} = \frac{\mathbf{M}^\top f_\theta(\mathbf{x}^q)}{\|\mathbf{M}\|_2 \|f_\theta(\mathbf{x}^q)\|_2}. \tag{10}$$

The softmax function σ maps the score, $\mathbf{v}$, to a probability distribution, $\mathbf{P}$, and an instance in the query set will be classified to the class with the highest probability.

4.5 Summary

FSL-based sensing has good scalability capacity. Whenever novel classes need to be added, a few samples of these classes should be collected and their feature representations can be generated with acceptable overheads. Let us revisit Fig. 2 for an analysis of cross-domain sensing. Data of the same class from the same domain is likely clustered, while data of different classes from different domains is likely separated away. The domain shift may result in the failure of cross-domain classification. In contrast, FewSense classifies the samples by comparing the samples in the support and query sets, while both sets are drawn from the same target domain. Therefore, the samples in both sets undergo the same domain shift. By using fine-tuning, we can rapidly adapt the feature extractor and classifier weights using a few samples from the support set, i.e., a transformation from the source domain to the target domain. This approach enables the model to adapt to the target domain with minimal effort.

5 Collaborative Sensing

In the previous sections, we introduced a Wi-Fi sensing system using one transmitter-receiver setup that can capture features from a particular direction. However, since the position and orientation of the user cannot be predicted, some transmitter-receiver links may not be optimal to capture CSI variations. The performance can be boosted by employing multiple receivers, which can enrich feature observations from different directions and work collaboratively to improve system robustness and classification accuracy. Multiple transmitters are not considered since the MAC layer

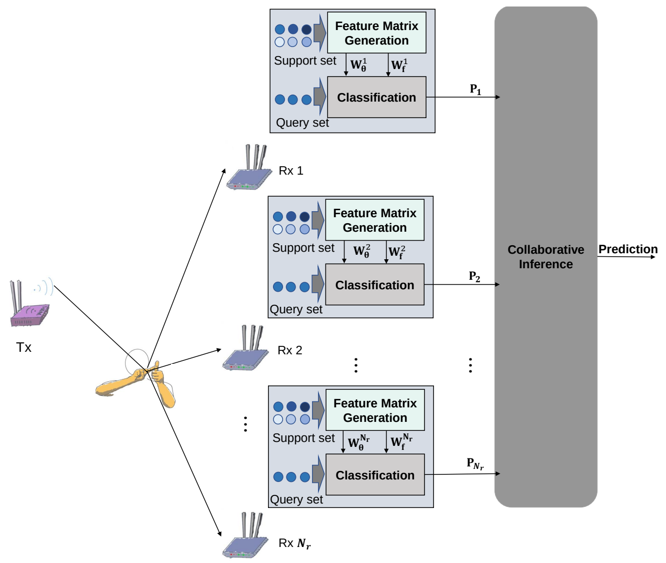

Fig. 6. Collaborative sensing using multiple receivers.

of Wi-Fi employs the CSMA protocol to prevent collisions. Multiple transmitters may cause uneven sampling, i.e., the received packets in the receiver may not be evenly distributed in time. Therefore, we consider one transmitter and multiple receivers in this paper. Besides, normal data traffic is not considered in this paper since it is not stable and may also cause uneven sampling or low sampling rate problems.

As demonstrated in Fig. 6, there are N_r receivers deployed for collaborative sensing. Each receiver will be equipped with the fine-tuning-FSL-based sensing approach introduced in Section 4. When a signal is sent by a transmitter, all the receivers will receive it simultaneously but from different directions. Each receiver will be initially deployed with the same feature extractor. For the i-th receiver, it can construct its own support set, $\mathbf{S}_i = (\mathcal{X}_i^s, \mathcal{Y}_i^s)$. The i-th receiver can then carry out fine tuning to adapt its feature extractor f_θ^i with weights $\mathbf{W}_\theta^i$ and the classifier with the weight matrix $\mathbf{W}_\mathrm{f}^i$.

In the classification stage, each receiver will also collect its own query set, $\mathbf{Q}_i$. The i-th receiver will first carry out the independent inference and obtain a probability distribution, $\mathbf{P}_i$. They will then work together by calculating an averaged probability distribution of all their observations, given as

$$\mathbf{P}^c = \frac{1}{N_r} \sum_{i=1}^{N_r} \mathbf{P}_i. \tag{11}$$

The class with the highest probability is predicted as the final decision.

The work in [36] reveals that the relative direction and location would have a major impact on the quality of CSI and would affect how well the sensing model performs. The receivers in collaborative sensing are placed in various places to obtain data from various relative directions and locations. By combining multiple observations together, the deep learning model can have a more comprehensive picture of the gestures.

TABLE 1
Summary of Datasets.

	Environment	User ID	# classes × # reps × # Rx	# samples
SignFi	Lab	User s5	276×20×1	5520
	Lab 2	User s1	150×10×1	1500
		User s2	150×10×1	1500
		User s3	150×10×1	1500
		User s4	150×10×1	1500
	Home	User s5	276×10×1	2760
Widar	Classroom	User w1	6×20×6	720
		User w2	6×20×6	720
		User w3	6×20×6	720
Wiar	Meeting room	User a1	16×30×1	480
		User a2	16×30×1	480
		User a3	16×30×1	480
		User a4	16×30×1	480
		User a5	16×30×1	480
		User a6	16×30×1	480

6 Experimental Evaluation

6.1 Setup of Experiments

6.1.1 Dataset

We used three public datasets for evaluation, i.e., SignFi [12], Widar 3.0 [21] and Wiar [26]. The three datasets were collected with real experiment settings in practical scenarios. The CSI of all these three datasets are collected by the Intel 5300 Wi-Fi NIC using the IEEE 802.11 CSI tool [34]. This tool reports the CSI of 30 subcarrier groups for each packet at 20 MHz channel spacing. The information in the three datasets is summarised in Table 1. The datasets are collected by different research groups. Thus, their volunteers and experimental experiments are different.

For each activity, we selected $U_s = 200$ packets to obtain a uniform input. There are 30 subcarrier groups in each packet, and each subcarrier has amplitude and phase information, thus $U_{ap} = 60$. Finally, there are three transmitter-receiver antenna pairs, i.e., $U_{ant} = 3$. Thus, we have the CSI tensors: $\mathbf{x} \in \mathbb{R}^{200\times60\times3}$.

SignFi dataset. The SignFi dataset [12] contains CSI samples of 276 different sign language gestures, which involve head, arm, hand, and finger movements. The gestures are performed by five users in three environments. Specifically, the user s5 performs all 276 sign language gestures at home and in a lab environment. Users s1 to s4 also carry out a subset of the gestures in the same lab room, but the settings vary, e.g., with different laptop placements and desk and chair arrangements. Hence, the lab environment for users s1 to s4, denoted as Lab 2 in this paper, is deemed different from the lab environment for user s5. User s5 performs 276 sign languages. Each class was performed 20 times in the lab and 10 times at home. Users s1 to s4 perform 150 sign languages 10 times in the lab 2 environment.

Widar dataset. The Widar dataset [21] is a large dataset, and we only used part of it. Specifically, we selected six gestures, namely Push & Pull, Sweep, Clap, Slide, Draw-Zigzag, and Draw-N. These gestures involve arm and hand movements. Six receivers are used to capture each gesture. We used data from three users, denoted as users w1, w2, and w3. Each user performs 6 gestures 20 times in a classroom environment.

Wiar dataset. The Wiar dataset [26] contains 16 different human motions, namely Horizontal Arm Wave, High Arm Wave, Two Hands Wave, High Throw, Draw X, Draw Tick, Toss Paper, Forward Kick, Side Kick, Bend, Hand Clap, Walk, Phone Call, Drink Water, Sit Down, and Squat. These activities involve torso, arm, and hand movements. We used the data of six users, denoted as a1 to a6, for our experiments. Each user performs each activity 30 times in a meeting room.

6.1.2 Training Configuration

The feature extractor was trained in a supervised learning manner. The data from the user s5 lab environment of the SignFi dataset was used as the base set. We used the Adam optimiser with an initial learning rate of $1e^{-3}$ to minimise the cross-entropy loss function. The learning rate was multiplied by 0.1 whenever the validation loss stopped decreasing for 20 epochs. The training process of the feature extractor terminated when the validation loss stopped decreasing for 50 epochs. All experiments were run on a PC with an i7-8700K 3.7 GHz CPU, and NVIDIA GeForce GTX 2080Ti with 16 GB memory. Tensorflow and Keras were used.

6.1.3 Evaluation Method

This paper evaluated the in-domain sensing (Section 6.2), cross-domain sensing (Section 6.3), cross-dataset sensing (Section 6.4), and collaborative sensing (Section 6.5). The base set was constructed by randomly selecting N_b classes each with K_b samples from the user s5 lab environment in the SignFi dataset. The feature extractor, denoted as $f_\theta^{N_b}$, was trained from scratch using the base set.

We randomly selected N different classes (ways) each with K samples (shots) from SignFi, Widar, or Wiar datasets to construct the support set $\mathbf{S}$. The remaining data of each selected class was used as the query set.

Classification accuracy and the confusion matrix were used as the metrics. Accuracy was defined as the number of correct predictions divided by the total number of predictions. The confusion matrix was used to show the number of correct and incorrect predictions.

6.1.4 Evaluation Scenarios

In order to evaluate the cross-domain capability of the FewSense, we have considered following five scenarios:

- **Scenario 1, In-domain Evaluation**: The support and query sets are from the user s5 lab environment, which is the same as the feature extractor pre-training environment.
- **Scenario 2, Cross-Environment Evaluation**: The support and query sets are from the user s5 home environment, i.e., the same user but different environments. As N_b = 200 classes are used for training the feature extractor, there are 76 remaining novel classes.
- **Scenario 3, Cross-Environment and Cross-User Evaluation**: The support and query sets are from users s1 to s4 in the lab 2 environment, i.e., different users and different environments. In the SignFi dataset, these four users performed 150 classes of sign language, and 25 of them were novel classes.
- **Scenario 4, Cross-dataset (Gesture recognition)**: the support and query set are from the Widar dataset (gesture recognition) in our experiments. The cross-dataset scenario is also a special case of the cross-domain. In this scenario, not only are the environments and users different, but the forms of the motions and devices are also different. The sign language and gesture recognition tasks are similar. Since the sign language contains movement of hands, arms, and head, and the gesture contains hands, and arms.
- **Scenario 5, Cross-dataset (Activity recognition)**: the support and query set are from the Wiar dataset (activity recognition) in our experiments. Human activities are completely different from sign language recognition since they are mostly torso motions.

6.2 In-Domain Sensing

In-domain sensing is evaluated in this section, i.e., the base set, support set, and query set share the same domain. Intuitively, a feature extractor will have better generalisation capability when more base classes are available. We used the data from the user s5 collected from the lab environment in the SignFi dataset as the base set. We trained feature extractors, $f_\theta^{N_b}$, with N_b base classes. Specifically, we studied N_b = 50, 100, 150, 200, and 250. These N_b classes were randomly selected from all the available classes, i.e., 276 classes in total. The rest of the classes of the user s5 lab environment were used to evaluate the feature extractor's novel class recognition performance. Fine-tuning was not applied. We evaluated different number of ways, i.e., N = 2 to 26, and one shot, i.e., K=1.

As shown in Fig. 7, a larger N_b, i.e., more base classes, leads to a higher accuracy, which is expected. When there are more novel classes in the support set, i.e., a higher N, the accuracy is decreasing, because it requires the feature extractor with better generalisation capability. Specifically, the average accuracies over all different numbers of novel classes are 97.9% and 99.2% when $N_b = 200$ and $N_b = 250$, respectively. However, if the number of base classes is less than the number of classes in the support set, the FewSense's performance suffers. For example, FewSense's performance can only reach accuracies of 30.3% and 36.0% when the number of base classes is 10 and 20, respectively, in the case of 1-shot 26-way learning. Therefore, the feature extractor should be trained with a higher number of classes in the base set than in the support set.

In the rest of this paper, we used f_θ^{200} as the feature extractor. To further evaluate the performance of the feature extractor f_θ^{200}, we increased the number of novel classes to 76. As shown in Table 2, the classification accuracy is 91.7% when $N = 76$, which is still high.

6.3 Cross-Domain Sensing

In this section, we evaluated the cross-domain sensing performance. The feature extractor f_θ^{200} is trained with the user s5 lab environment but the support and query sets are from different domains.

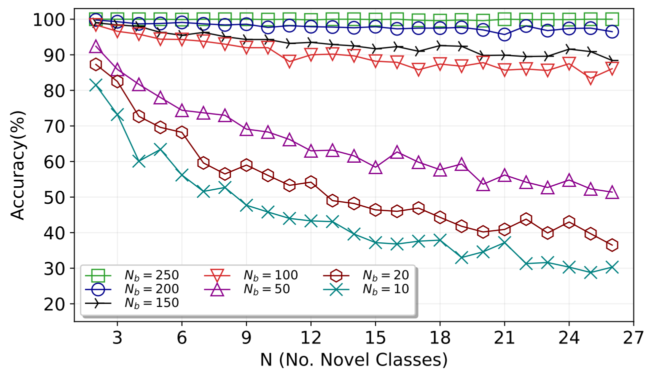

Fig. 7. Impact of the number of base classes.

TABLE 2
In-Domain Sensing Performance of the Feature Extractor f_θ^{200}.

# ways	30	40	50	60	70	76
Accuracy	95.4%	95.8%	95%	93.3%	92.3%	91.7%

6.3.1 Impact of Numbers of Novel Classes

We evaluated N-way 1-shot learning with direct feature matrix generation. Only the data of novel classes was used, hence we evaluated $N = 2$ to 76 and $N = 2$ to 25 for scenarios 2 and 3, respectively.

As shown in Fig. 8, the accuracies of both scenarios decrease when the number of novel classes, N, is increasing, as a better generalisation capability of the feature extractor is required. The accuracy of scenario 2 dropped to 57.9% when $N = 76$. Regarding scenario 3, the results in Fig. 8b demonstrate that the system can learn the distinctive representation of the novel classes, even though the feature extractor has never seen data from these environments and users before. The accuracies vary for different users because each user may perform the same sign language in a different manner, which results in different data distribution. In addition, the performance of FewSense decreases as the number of novel classes in the support set increases. The reason behind this is that the more classes in the support set, the higher the probability that there are more classes that have similar features. This can also be observed in Fig. 2, where some classes in the same domain could be close together.

6.3.2 Impact of Numbers of Shots

This section studied the impacts of different numbers of shots, K, in the support set. Fine-tuning was not used. We increased K from 1 to 5 for both scenarios 2 and 3.

The results are shown in Fig. 9, the overall performance of FewSense increased as the number of shots increased. For scenario 1, we used all the remaining 76 classes, i.e., 76-way K-shot. The accuracy increased from 57.9% to 71.5% when K increased from 1 to 5 (shown by the orange line). Regarding scenario 3, we tested 25-way K-shot. Increasing the number of shots can enrich the data diversity in the support set, thus increasing the generalisation capability of the feature extractor. Therefore, the decrease in accuracy due to the number of new classes increase can be compensated by increasing the number of shots. Again, the accuracies vary according to different users, about 20% difference

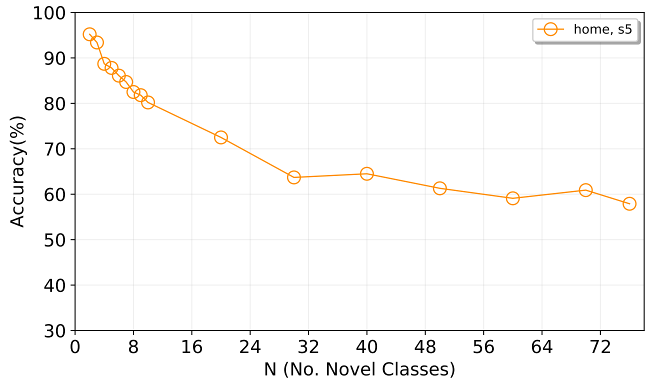

(a)

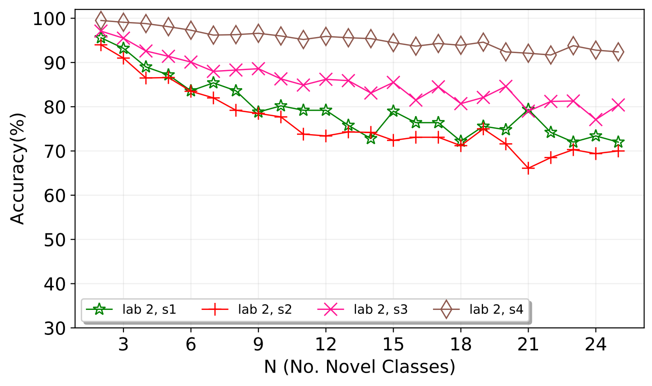

(b)

Fig. 8. Performance of cross-domain sensing. Impact of number of novel classes. Fine-tuning is not applied. The feature extractor f_θ^{200} is used. (a) Scenario 1, Cross-Environment Evaluation. (b) Scenario 2, Cross-Environment and Cross-User Evaluation.

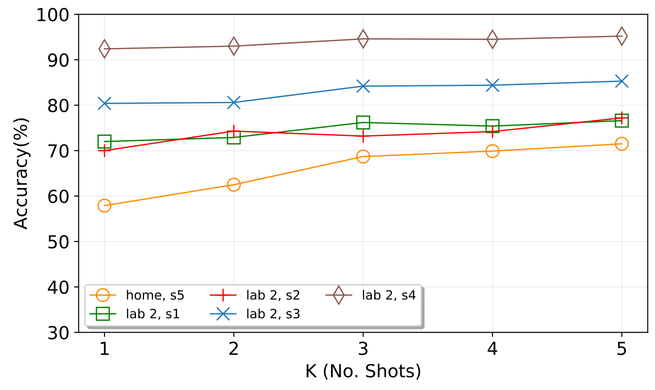

Fig. 9. Performance of cross-domain sensing. Impact of number of shots in scenario 1 (user s5) and scenario 2 (user s1-s4). Fine-tuning is not applied. The feature extractor f_θ^{200} is used.

between the best and worst cases, probably due to various gesture patterns among users. Note that user s5 had the lowest accuracy compared to the other four users, because the number of novel classes of user s5 was higher ($N_b = 76$).

6.3.3 Impact of Fine-Tuning

We performed fine-tuning on the support set with only one and five samples for each novel class. We studied 76-way 1-shot and 25-way 1-shot for scenarios 2 and 3, respectively.

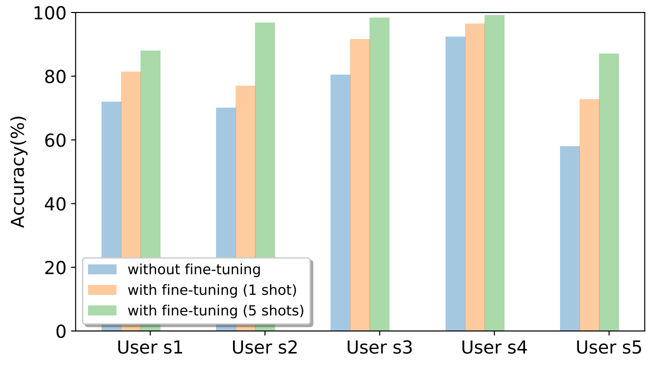

Fig. 10. Performance of cross-domain sensing. Impact of fine-tuning in scenario 1 (user s5) and scenario 2 (user s1-s4). The feature extractor f_θ^{200} is used.

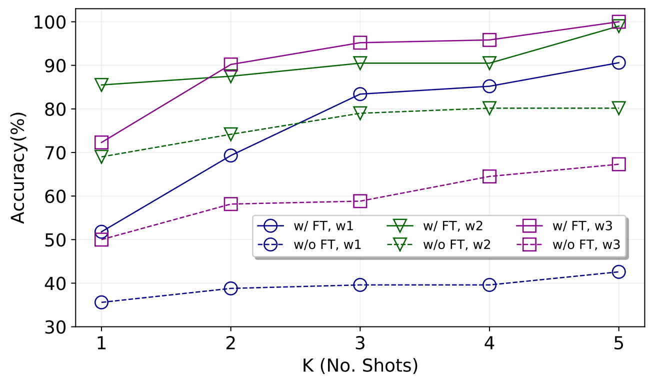

Fig. 11. Cross-dataset evaluation on the Widar dataset. The feature extractor f_θ^{200} is trained using SignFi dataset.

As shown in Fig. 10, fine-tuning has improved FewSense's performance for all the testing scenarios. For scenario 1 (user s5), the accuracy improved from 57.9% to 72.8% and 87.1%, when one shot and five shots were applied, respectively. For scenario 3 (users s1 to s4), the performance was improved by 8% and 16.9% on average when one and five shots were applied, respectively. The evaluation results indicated that our proposed fine-tuning method could significantly improve the cross-domain's accuracy and quickly adapt to the new domain without requiring extensive data collection, because the feature extractor can be updated even using one shot.

Compared to the direct matrix generation method, the fine-tune matrix generation can improve the performance of the FewSense significantly. The average accuracy improved from 75.5% to 83.8% and 81.2% to 93.9% for one and five shots learning, respectively. Therefore, the decrease in accuracy due to the new class increase can also be compensated by fine-tuning adjustments.

6.4 Cross-Dataset Evaluation

This section evaluated the classification performance when the base set and support & query sets were from different datasets. The same feature extractor f_θ^{200} trained on the SignFi dataset was used. The support and query sets were from the Widar or Wiar datasets.

This would be quite challenging. Firstly, there will be a significant domain shift between the datasets as the users and environments are different. Secondly, different datasets have different sensing tasks, which result in totally different CSI variation features. For example, sign languages in SignFi are mainly a combination of finger, hand, and head movements; the gestures in the Widar dataset involve hand movements, and the human motions in the Wiar dataset are large-scale human activities that involve arm, hand, limb, and leg, etc. The tasks of SignFi and Widar are similar, but the ones between SignFi and Wiar are quite different.

6.4.1 Evaluation on Widar Dataset

This section evaluated the recognition performance when the tasks of the base sets (SignFi) and the support & query sets (Widar) were different but similar. Specifically, the gesture data in the Widar dataset was used for evaluation.

As there are multiple receivers available in Widar, we selected the data of one receiver from users w1, w2, and w3. We evaluated a 6-way K-shot, where K = 1 to 5. We studied both direct feature matrix generation and fine-tuned feature matrix generation. The results are shown in Fig. 11.

When fine-tuning was used, the overall accuracy increased dramatically. The minimum accuracy increase was around 16.5%, when the data was from the users w1 and w2 in the one-shot learning case. The overall accuracy increased with an increase in the number of shots. In the case of one-shot learning with fine-tuning, the accuracies were 51.8%, 86.3%, and 72.3%, for user w1, w2, and w3, respectively. The five shots learning gave the best performance, i.e., 90.6%, 99.0% and 100% for user w1, w2, and w3, respectively. Comparing to the direct feature matrix generation, the average accuracy for five shots learning case was increased from 63.4% to 96.5%. The corresponding confusion matrix is shown in Fig. 12. The experiment results showed that our proposed method can be scaled to similar sensing tasks, e.g., gesture recognition, with only a few samples.

As the feature extractor was trained using the data of sign languages (SignFi), some latent features learned may not apply to gesture recognition (Widar). The performance was thus limited when fine-tuning was not used. When fine-tuning was used, even with very few samples, the recognition accuracy was significantly improved. This is because the feature extractor already has informative knowledge about how to extract latent features for sign language, and sign languages share some common features with gestures.

6.4.2 Evaluation on Wiar Dataset

This section evaluated the recognition performance when the tasks of the base sets (SignFi) and the support & query sets (Wiar) are quite different. Specifically, the human activity data in the Wiar dataset was used for evaluation.

We selected the data from six users in the Wiar dataset. We evaluated 16-way K-shot, where K = 1 to 5. The experiments were conducted with fine-tuning applied. The experiment results are demonstrated in Fig. 13. The feature extractor f_θ^{200} achieved the highest accuracy for user a1, with an accuracy of 66.2% and 94.2% for one and five shots learning, respectively. The lowest accuracy was shown for user a3, with an accuracy of 31.0% and 57.2% for one

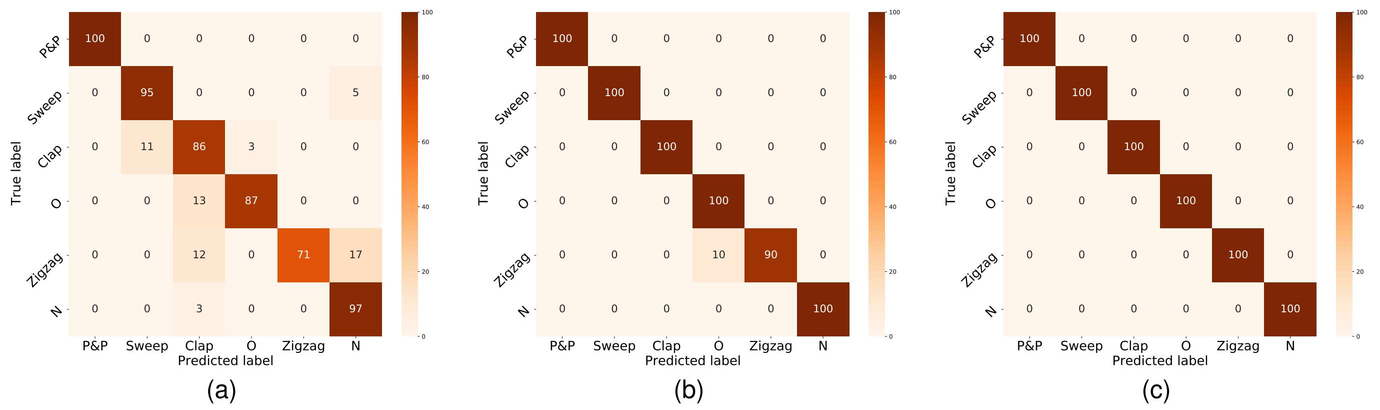

Fig. 12. Cross-dataset evaluation on the Widar dataset. The confusion matrix for 5 shots learning. (a) User w1. (b) User w2. (c) User w3.

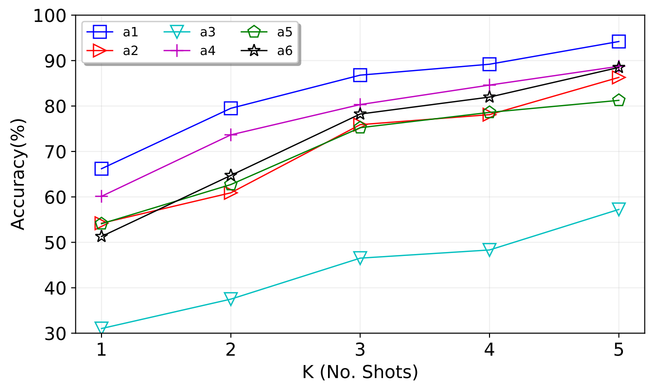

Fig. 13. Cross-dataset evaluation on the Wiar dataset. The feature extractor f_θ^{200} is trained using SignFi dataset.

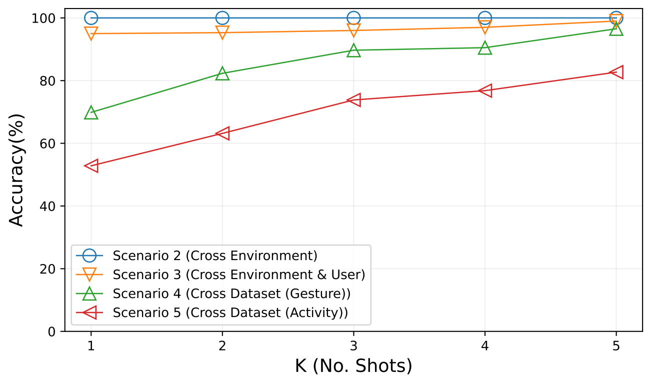

Fig. 14. Performance comparison of FewSense in different scenarios with various domain differences.

and five shots learning, respectively. In the case of five-shot learning, the performance of FewSense was 82.7% of accuracy on average. The results demonstrate that our feature extractor can adapt to various sensing tasks without the burden of high data collection and model retraining, even when the tasks are very different from the original task. FewSense's performance was shown differently to different users. There may be many reasons behind this. One could be that different users perform the activities in unique ways, which would result in different domain shifts. A larger domain shift in comparison to the original feature extractor training domain may require more data to generalise.

6.4.3 *Impact of the Sample Size in Cross-domain Scenarios*

In this section, we investigated how domain difference affects the FewSense's performance. As indicated in the Section 6.1.4, the domain difference between feature extractor training and evaluation increases from scenario 2 to 5. To ensure a fair comparison, we set the number of novel classes to six and employed a fine-tuned feature matrix generation approach.

As shown in Fig. 14, scenario 2 with the smallest domain difference exhibits the best performance, as it achieved around 100% accuracy throughout various numbers of shots. When the number of shots remained constant, FewSense's performance declined as the domain difference increased. Therefore, while applying FewSense in cross-domain scenarios, we need to take into account the difference between the source domain and the evaluation domain. More support set samples will be required when the domain difference is more significant.

6.4.4 *Discussion*

The work [23] also used FSL for Wi-Fi sensing and argued it is cumbersome to build a feature extractor with good generalisation capability. Hence they designed virtual gesture generation to reduce the effort of collecting data.

However, as we showed in this section, we can leverage the public dataset as the base set and train a versatile feature extractor. When the feature extractor is applied to a different sensing task, we can always fine-tune the feature extractor using very few samples from the new task. Therefore, the overhead for collecting the base set can be mitigated.

Moreover, we evaluated the cross-dataset performance of FewSense with 6-way and 16-way learning on the Widar (Section 6.4.1) and Wiar datasets (Section 6.4.2), respectively. Even though cross-dataset sensing tasks are more challenging, the FewSense has higher accuracy on them when compared to cross-domain evaluations in Section 6.3. This is due to the fact that in Section 6.3 we evaluated FewSense with up to 76-way. There are more novel classes in Section 6.3 than there are in this section. The overall accuracy is decreasing as more novel classes are added, as demonstrated in Fig. 8.

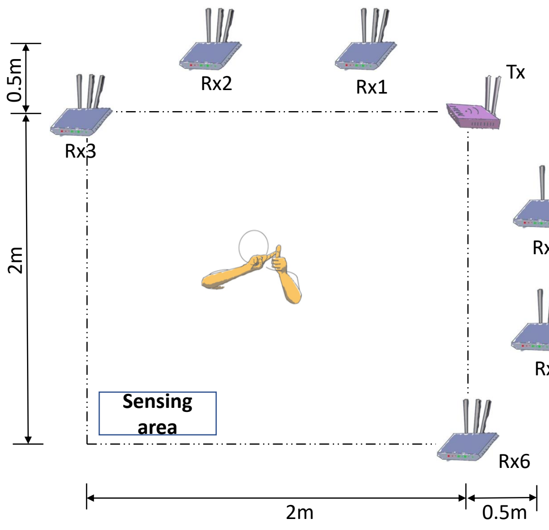

Fig. 15. The deployment of receivers in the Widar dataset.

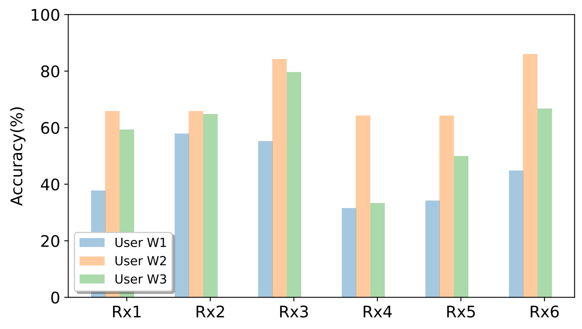

Fig. 16. One shot performance of FewSense with a single receiver. The feature extractor f_θ^{200} is trained using the SignFi dataset. Support and query sets are from Widar dataset.

Therefore, it is reasonable that FewSense has better accuracy in this section.

6.5 Collaborative Sensing

In this section, we evaluated the performance of the collaborative sensing algorithm. The fine-tuning was applied in this section. The same feature extraction, f_θ^{200}, trained on the SignFi dataset was used. The support and query sets were from users w1, w2 and w3 of the Widar dataset. Six gestures were performed 20 times and captured by six receivers each time. Each receiver has 20 samples for each gesture. We constructed the support and query sets for each receiver. One to five samples were randomly selected and added to the support set, and the remaining were used as the query set.

The deployment of receivers is shown in Fig. 15. The performance of FewSense with each receiver is shown in Fig. 16. The receiver 3 achieved the best performance among all the receivers, and the receiver 6 achieved comparable performance to the receiver 3. It should be noted that receivers 3 and 6 perform best. The reason behind this could be that receivers 3 and 6 have better locations, in which case the model can be adapted to a new domain easier compared to other receivers.

Due to the fact that the deployment of the receivers may impact the performance of the collaborative sensing system, we evaluate the performance of the collaborative sensing system using the average accuracy of all possible receiver combination sets. Accuracy can be improved by using multiple receivers and more shots. Exploiting more receivers enables the feature extractor to view gestures from different directions, so rich features can be obtained for improving system performance. As shown in Fig. 17, the accuracy of the FewSense can be boosted by using multiple receivers. Specifically, for one-shot learning, when the number of receivers increased from 1 to 6, the accuracy of user w1, w2, and w3 improved by 38.6%, 18.3%, and 30.8%, respectively. Comparing to the one receiver case, the average accuracy was increased by 29.2% when six receivers were used. Similarly, the classification accuracy in collaborative sensing can also be enhanced by more shots. For one receiver case, the accuracy was improved by 39.2%, 17.2% and 30.1% for user w1, w2 and w3, respectively, when the number of shots was increased from 1 to 5. The highest accuracy is 100.0% achieved by the 5-shot learning using six receivers. As the more samples involved in the fine-tuning, the better generalisation capability that feature extractor can obtain.

The work in [23] also used multiple receivers. However, the accuracy of their work is already relatively high with only one receiver, so the accuracies were saturated with more receivers. However, as demonstrated by our work, more receivers will be beneficial when the accuracy achieved using a single receiver is not saturated.

6.6 Complexity

The computational overhead involves three parts: feature extractor training, fine-tuning, and inference. The signal pre-processing algorithm used in all three stages took 0.3 seconds.

Training a feature extractor probably is the most computationally expensive. In order to achieve good generalisation capability, the feature extractor needs to be pre-trained with a large number of base classes. Specifically, we trained the feature extractor using 200 classes, each with 20 samples of the user s5 lab environment in the SignFi dataset, which took around 10 minutes. Fortunately, the feature extractor only needs to be trained once and can be done offline. The pre-trained feature extractor takes up 45 MB of storage, which can be deployed on embedded systems.

Fine-tuning is applied for adapting the pre-trained feature extractor and classifier to new sensing tasks or domains. The time cost depends on the amount of data. In all the experiments studied in this paper, the most time-consuming one is 76-way 5-shots learning, which takes 82 seconds, which is deemed acceptable.

Inference is completed by the proposed collaborative sensing model when multiple receivers are available. The time consumption of each inference is around 0.04 seconds, which can be done almost in real-time.

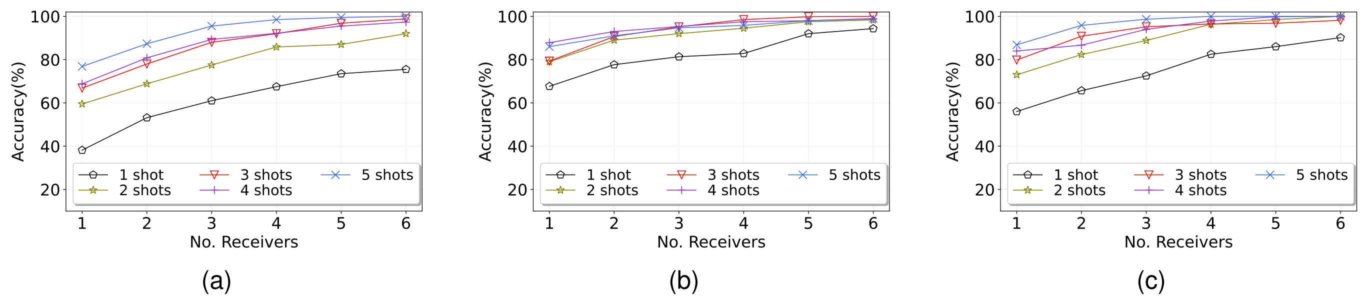

Fig. 17. Performance of collaborative sensing using multiple receivers and different number of shots. The feature extractor f_{θ}^{200} is trained using the SignFi dataset. Support and query sets are from the Widar dataset. (a) User w1. (b) User w2. (c) User w3.

6.7 Comparison with the-State-of-the-Art

6.7.1 Comparison with Domain Adversarial Training

This section compared the performance of the proposed method to a state-of-the-art domain adversarial training-based method, also known as adversarial domain adaptation, which has been employed in the Wi-Fi sensing area, e.g., [18], [19].

The basic idea of domain adversarial training is to train a network on data from different domains, which are termed source domains. A domain adversarial network includes a feature extractor, a classifier, and a domain discriminator. The feature extractor is used to extract features. The classifier is used to identify the label of the input. The domain discriminator is used to distinguish the domain label of the input. The domain discriminator would force the feature extractor to extract domain-independent features. After training, the network is expected to perform well on target domain data.

To ensure a fair comparison, we used the same modified AlexNet architecture in this paper as the feature extractor of the adversarial network. We trained the model with data from two different environments, i.e., lab and lab 2, and five users of the SignFi dataset. Each environment and user pair forms a source domain. The data from the home environment, user s5, was used as the target domain data.

The comparison results are shown in Table 3. The domain adversarial training-based approach only achieved an overall accuracy of 4%, which failed to recognise the sign language gestures in the target domain. This is probably because the domain adversarial network requires a large number of domains to enable the feature extractor to learn domain-independent features. For example, the work in [19] revealed their classification accuracy increased from about 45% to 75% when the number of source domains was increased from 2 to 22.

Instead of training a feature extractor to learn the domain-independent features, our proposed method adapts to the target domain by comparing the similarity of the extracted features between target domain instances. With one sample from each class, our method achieved 57.9% accuracy without fine-tuning. The accuracy can be further increased to 72.8% when fine-tuning is applied.

TABLE 3
Performance Comparison With Domain Adversarial Training

Methods	Accuracy
FewSense without fine-tuning (1-shot)	57.9%
FewSense with fine-tuning (1-shot)	72.8%
Domain adversarial training	4.0%

TABLE 4
Cross-Domain Performance Comparison With Widar

Methods	User w1	User w2	User w3
Widar	82.0%	90.5%	92.4%
FewSense (1-shot 6-Rx)	76.0%	94.3%	90.2%
FewSense (2-shot 6-Rx)	92.0%	98.3%	100%
FewSense (5-shot 2-Rx)	87.3%	91.0%	95.8%

6.7.2 Comparison with Domain-Independent Feature-based Approach

The work in [21] proposed BVP, a domain-independent feature, to address the cross-domain sensing problem. According to [21], extracting BVP requires at least three receivers. The Widar dataset provides BVP extracted from six receivers, which is used here for comparison. We used the same deep learning model in [21]. In order to perform cross-domain sensing, the BVP data of users w4 to w9 collected from the hall and office environments was used for training. The BVP data of users w1 to w3 obtained from the classroom was used for evaluation. In comparison, we evaluated the performance of the collaborative sensing method on data from the same three users collected in the same classroom environment via six receivers.

The BVP-based approach achieved an average accuracy of 82.0%, 90.5% and 92.4% for the user w1, w2 and w3, respectively, using six receivers. The applications of the BVP feature may be limited in real life since they require at least three receivers to resolve the ambiguity problem. Comparatively, our FewSense model can outperform the BVP-based approach only with two receivers, with respective results of 87.3%, 91.0%, and 95.8% for users w1, w2, and w3. The hardware constraint can be reduced since our collaborative sensing model can achieve better performance with only two receivers. In the case of six receivers for collaborative sensing method, as can be observed from Table 4, one-shot learning can achieve comparable performance with the BVP-based method. When two shots are used, our method outperforms the BVP-based method by an average accuracy of 8%.

In terms of complexity, BVP feature extraction is computationally expensive. For example, it took around 205 seconds to compute the BVP feature for one gesture from six receivers in the classification stage. The high computational

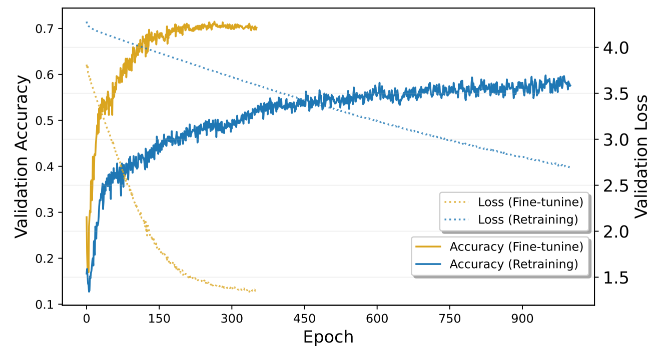

Fig. 18. Comparison of fine-tuning and retraining.

complexity limits its practical use. In comparison, the total time cost for collaborative sensing with six receivers is 0.24 seconds. As a result, the classification of FewSense can be done in real-time.

6.7.3 Comparison with Classic Supervised-learning-based Sensing Method

Fig. 18 depicts a comparison of the convergence speed for FewSense and retraining the entire network. The number of shots per class was fixed at 1, and the training procedure was terminated after the validation loss stopped decreasing for 20 epochs. For FewSense, the pre-trained feature extractor f_θ^{200} was utilised. FewSense can adapt to a new environment far faster than retraining a network. The typical re-training technique converges substantially slower than the suggested method with the same quantity of data. Validation accuracy and loss of fine-tuning converge quicker than retraining. Furthermore, the fine-tuning approach can attain approximately 70% accuracy, whereas the retraining method's greatest accuracy was 58%. Thus, with the same amount of data, the FewSense can achieve higher accuracy with less computational overhead compared to the classic deep learning-based sensing method.

7 Related Work

7.1 Few-Shot Learning

The FSL has been successfully implemented in many vision-based tasks [37] and the similarity-based methods are widely investigated. Matching networks [22] is proposed to use a cosine similarity function to solve the FSL problem. The authors in [38] train a neural network with a large number of base classes and then replace the last fine-tuning layer with a cosine similarity function. Researchers in [39] proposed a prototypical network (PN) for FSL, which employs Euclidean distance as the distance metric. The works above aim to learn transferable features and a fixed similarity function, but the generalisation capability of them is limited. The work in [40] proposed relation network with a trainable similarity metric to address the above limitation.

7.2 Domain Robustness of Wi-Fi Sensing

The authors in [18], [19] use a domain-adversarial training-based domain adaptation method to extract domain-independent features from multiple domains. For example, the work in [18] employs a gesture classifier to classify gestures, and a domain discriminator to recognise the domain label of the input samples. The feature extractor is trained to cheat the domain discriminator such that the domain discriminator cannot distinguish the domain labels of the input. The feature extractor is expected to map the input from different domains to the same feature space. However, this method requires a massive number of training samples from different domains to obtain satisfactory performance.

Transfer learning focuses on leveraging the knowledge of a pre-trained model and applying the model to a different but similar task. In order to reduce the model retraining effort in the target domain, the authors in [20] propose a transfer learning-based method called CrossSense, which employs an ANN-based model to translate the CSI features of gestures in the source domain to the target domain. Although transfer learning can reduce the data collection effort in a new domain, it still requires many data samples from the target domain to achieve a satisfying performance. Moreover, transfer learning only works when the source and target domains are similar enough. Otherwise, the problem of negative transfer may limit the applications of this method [41].

The domain-independent feature-based method is another type of solution. Widar [21] uses multiple receivers to extract BVP. However, at least three receivers are required to resolve the velocity direction ambiguity problem, and the feature extraction overhead cannot be ignored. Those factors may limit the application in real deployments.

The work in [10] extracts the motion patterns as the input features, which are experimentally demonstrated to be domain-independent. However, some similar gestures could have similar movement patterns. Therefore, the classes of the gestures need to be designed to avoid similarity.

8 Conclusions and Future Works

8.1 Conclusions

This paper proposed FSL-based WiFi sensing, i.e., FewSense, to address the scalability and domain-dependent challenges. FewSense utilised a revised AlexNet architecture as the feature extractor to gain generalisation capability. The features of the query and support sets were compared, and the inference was made based on their cosine similarity score. Collaborative sensing was designed to fuse observations from multiple receivers to boost classification accuracy. Three public Wi-Fi sensing datasets, including SignFi (sign language), Widar (gesture recognition) and Wiar (human activity recognition), were leveraged for evaluation. We carried out an extensive evaluation using a feature extractor trained on the SignFi dataset. The experimental results indicated that FewSense could be adapted to new sensing tasks or domains with low data collection and computational costs. The FewSense with one-shot learning can recognise novel sign language gestures in SignFi with an average accuracy of 99.2% and 84.2% in in-domain and cross-domain scenarios, respectively. When applying FewSense to new sensing tasks, FewSense recognised novel gestures on the Widar dataset with an average accuracy of 69.9% and 96.5% for one-shot and five-shot learning, respectively. It also achieved an average accuracy of 52.8% and 82.7% for one-shot and five-shot learning, respectively, for classifying novel human activities on the Wiar dataset. Finally, our collaborative sensing approach can boost the classification accuracy by 30% on average when there were six receivers. In summary, FewSense demonstrated that cross-dataset sensing is applicable. The generalisability of the feature extractor can be achieved using a publicly available dataset, alleviating the overhead of data collection.

8.2 Future Works

In real-world applications, Wi-Fi sensing systems are typically employed in complicated electromagnetic environments, where co-channel interference could be caused by other devices using the same frequency band, such as Bluetooth and ZigBee. This problem was studied in [42] for traditional machine learning models. The researchers proposed two subcarrier selection algorithms that dynamically pick subcarriers based on correlation changes rather than merely fusing subcarriers. They effectively improve the robustness of the Wi-Fi sensing model under interference scenarios. However, further studies are required for deep learning based methods.

Although collaborative sensing can boost the performance of FewSense, it is limited by the number of deployed receivers. We aim to further improve the system's performance through data augmentation, which can enrich the training dataset. These two approaches can be used together, as data augmentation is applied to the training stage while collaborative sensing is used at the classification stage.

Finally, WiFi sensing requires CSI, and several drivers provide CSI, including Nexmon CSI[2], Intel NIC 5300 [43] and Atheros 9580 [32]. With the advancement of Wi-Fi sensing, the IEEE 802.11 working group has created a new task group named IEEE 802.11bf to develop a new amendment to the Wi-Fi standard that would offer enhanced sensing capabilities. Indeed, the majority of the existing works rely on Intel NIC 5300 and Atheros 9580. Alternatively, we will build our own testbed utilising low-cost ESP32 and Raspberry Pi and investigate how Wi-Fi sensing systems can collaborate across many platforms, allowing for the cost-effective implementation of collaborative sensing.

References

[1] J. Liu, H. Liu, Y. Chen, Y. Wang, and C. Wang, "Wireless sensing for human activity: A survey," *IEEE Commun. Surveys Tuts.*, vol. 22, no. 3, pp. 1629–1645, Aug. 2020.

[2] I. Nirmal, A. Khamis, M. Hassan, W. Hu, and X. Zhu, "Deep learning for radio-based human sensing: Recent advances and future directions," *IEEE Commun. Surveys Tuts.*, vol. 23, pp. 995 – 1019, Feb. 2021.

[3] Y. Wang, J. Liu, Y. Chen, M. Gruteser, J. Yang, and H. Liu, "E-eyes: device-free location-oriented activity identification using fine-grained WiFi signatures," in *Proc. 20th Annual Int. Conf. Mobile Computing and Networking (MobiCom)*, Maui, Hawaii, Sep. 2014, pp. 617–628.

[4] B. Li, W. Cui, W. Wang, L. Zhang, Z. Chen, and M. Wu, "Two-Stream convolution augmented transformer for human activity recognition," in *Proc. AAAI Conf. Artif. Intell. (AAAI)*, held virtually, May 2021, pp. 286–293.

2. https://github.com/seemoo-lab/nexmon_csi

[5] F. Wang, W. Gong, and J. Liu, "On spatial diversity in Wi-Fi-based human activity recognition: A deep learning-based approach," *IEEE Internet Things J.*, vol. 6, no. 2, pp. 2035–2047, Sep. 2018.

[6] H. Wang, D. Zhang, Y. Wang, J. Ma, Y. Wang, and S. Li, "RT-Fall: A real-time and contactless fall detection system with commodity Wi-Fi devices," *IEEE Trans. Mobile Comput.*, vol. 16, no. 2, pp. 511–526, Apr. 2016.

[7] L. Zhang, Z. Wang, and L. Yang, "Commercial Wi-Fi based fall detection with environment influence mitigation," in *Proc. Annu. IEEE Int. Conf. Sens. Commun. Netw. (SECON)*, Massachusetts, USA, Jun. 2019, pp. 1–9.

[8] W. Wang, A. X. Liu, and M. Shahzad, "Gait recognition using Wi-Fi signals," in *Proc. ACM Int. Jt. Conf. Pervasive Ubiquitous Comput.(Ubicomp)*, New York, NY, USA, Sep. 2016, p. 363–373.

[9] L. Zhang, C. Wang, M. Ma, and D. Zhang, "WiDIGR: Direction-independent gait recognition system using commercial Wi-Fi devices," *IEEE Internet Things J.*, vol. 7, no. 2, pp. 1178–1191, Nov. 2019.

[10] C. L. Li, M. Liu, and Z. Cao, "WiHF: Gesture and user recognition with Wi-Fi," *IEEE Trans. Mobile Comput.*, vol. 21, pp. 1–1, Jul. 2020.

[11] R. Gao, M. Zhang, J. Zhang, Y. Li, E. Yi, D. Wu, L. Wang, and D. Zhang, "Towards position-independent sensing for gesture recognition with Wi-Fi," *Proc. ACM Interact. Mob. Wearable Ubiquitous Technol.*, vol. 5, no. 2, pp. 1–28, Jun. 2021.

[12] Y. Ma, G. Zhou, S. Wang, H. Zhao, and W. Jung, "SignFi: Sign language recognition using Wi-Fi," *Proc. ACM Interact. Mob. Wearable Ubiquitous Technol.*, vol. 2, no. 1, pp. 1–21, Mar. 2018.

[13] J. Shang and J. Wu, "A robust sign language recognition system with sparsely labeled instances using Wi-Fi signals," in *Proc. Int. Conf. Mob. Ad Hoc Sens. Syst. (MASS)*, Orlando, FL, USA, Oct. 2017, pp. 99–107.

[14] Y. Zeng, D. Wu, J. Xiong, J. Liu, Z. Liu, and D. Zhang, "Multisense: Enabling multi-person respiration sensing with commodity Wi-Fi," *Proc. ACM Interact. Mob. Wearable Ubiquitous Technol.*, vol. 4, no. 3, pp. 1–29, Sep. 2020.

[15] H. Wang, D. Zhang, J. Ma, Y. Wang, Y. Wang, D. Wu, T. Gu, and B. Xie, "Human respiration detection with commodity Wi-Fi devices: do user location and body orientation matter?" in *Proc. ACM Int. Jt. Conf. Pervasive Ubiquitous Comput. (Ubicomp)*, Heidelberg, Germany, Sep. 2016, pp. 25–36.

[16] A. Goldsmith, *Wireless Communications*. Cambridge University Press, 2005.

[17] A. Krizhevsky, I. Sutskever, and G. E. Hinton, "Imagenet classification with deep convolutional neural networks," *Adv. Neural Inf. Process. Syst.*, vol. 25, no. 6, pp. 1097–1105, May 2012.

[18] H. Kang, Q. Zhang, and Q. Huang, "Context-aware wireless based cross domain gesture recognition," *IEEE Internet Things J.*, vol. 8, no. 17, Mar. 2021.

[19] W. Jiang, C. Miao, F. Ma, S. Yao, Y. Wang, Y. Yuan, H. Xue, C. Song, X. Ma, D. Koutsonikolas *et al.*, "Towards environment independent device free human activity recognition," in *Proc. Annu. Int. Conf. Mob. Comput. Netw. (MOBICOM)*, New Delhi, India, Oct. 2018, pp. 289–304.

[20] J. Zhang, Z. Tang, M. Li, D. Fang, P. Nurmi, and Z. Wang, "CrossSense: Towards cross-site and large-scale Wi-Fi sensing," in *Proc. Annu. Int. Conf. Mob. Comput. Netw. (MOBICOM)*, New York, NY, USA, Oct. 2018, pp. 305–320.

[21] Y. Zhang, Y. Zheng, K. Qian, G. Zhang, Y. Liu, C. Wu, and Z. Yang, "Widar3.0: Zero-effort cross-domain gesture recognition with Wi-Fi," *IEEE Trans. Pattern Anal. Mach. Intell.*, pp. 1–1, Aug. 2021.

[22] O. Vinyals, C. Blundell, T. Lillicrap, D. Wierstra *et al.*, "Matching networks for one shot learning," *Adv. Neural Inf. Process. Syst.*, vol. 29, pp. 3630–3638, Dec. 2016.

[23] R. Xiao, J. Liu, J. Han, and K. Ren, "OneFi: One-shot recognition for unseen gesture via COTS Wi-Fi," in *Proc. Conf. Embed. Networked Sens. (SenSys)*, Coimbra, Portugal, Nov. 2021, pp. 206–219.

[24] S. Ding, Z. Chen, T. Zheng, and J. Luo, "RF-net: A unified meta-learning framework for RF-enabled one-shot human activity recognition," in *Proc. Conf. Embed. Networked Sens. (SenSys)*, Virtual Event, Nov. 2020, pp. 517–530.

[25] J. Yang, H. Zou, Y. Zhou, and L. Xie, "Learning gestures from Wi-Fi: A siamese recurrent convolutional architecture," *IEEE Internet Things J.*, vol. 6, no. 6, pp. 10 763–10 772, Jun. 2019.

[26] L. Guo, L. Wang, C. Lin, J. Liu, B. Lu, J. Fang, Z. Liu, Z. Shan, J. Yang, and S. Guo, "WiAR: A public dataset for Wi-Fi-based activity recognition," *IEEE Access*, vol. 7, pp. 154 935–154 945, Oct. 2019.

[27] W. Wang, A. X. Liu, M. Shahzad, K. Ling, and S. Lu, "Understanding and modeling of Wi-Fi signal based human activity recognition," in *Proc. Annu. Int. Conf. Mob. Comput. Netw. (MOBICOM)*, Sep. 2015, pp. 65–76.

[28] Y. Ma, S. Arshad, S. Muniraju, E. Torkildson, E. Rantala, K. Doppler, and G. Zhou, "Location-and person-independent activity recognition with Wi-Fi, deep neural networks, and reinforcement learning," *ACM Trans. IOT.*, vol. 2, no. 1, pp. 1–25, Jan. 2021.

[29] J. Zhang, F. Wu, B. Wei, Q. Zhang, H. Huang, S. W. Shah, and J. Cheng, "Data augmentation and dense-lstm for human activity recognition using wi-fi signal," *IEEE Internet Things J.*, vol. 8, no. 6, pp. 4628–4641, Sep. 2020.

[30] Y. Wang, K. Wu, and L. M. Ni, "WiFall: Device-free fall detection by wireless networks," *IEEE Trans. Mobile Comput.*, vol. 16, no. 2, pp. 581–594, Apr. 2016.

[31] L. Van der Maaten and G. Hinton, "Visualizing data using t-SNE," *J. Mach. Learn. Res.*, vol. 9, no. 11, 2008.

[32] Y. Xie, Z. Li, and M. Li, "Precise power delay profiling with commodity Wi-Fi," *IEEE Trans. Mob. Comput.*, vol. 18, no. 6, pp. 1342–1355, Jul. 2018.

[33] X. Wang, L. Gao, and S. Mao, "CSI phase fingerprinting for indoor localization with a deep learning approach," *IEEE Internet Things J.*, vol. 3, no. 6, pp. 1113–1123, Dec. 2016.

[34] D. Halperin, W. Hu, A. Sheth, and D. Wetherall, "Tool release: Gathering 802.11n traces with channel state information," *ACM. SIGCOMM. CCR.*, vol. 41, no. 1, p. 53, Jan. 2011.

[35] R. Ranjan, C. D. Castillo, and R. Chellappa, "L2-constrained softmax loss for discriminative face verification," *arXiv preprint arXiv:1703.09507*, 2017.

[36] K. Niu, F. Zhang, X. Wang, Q. Lv, H. Luo, and D. Zhang, "Understanding Wi-Fi signal frequency features for position-independent gesture sensing," *IEEE Trans. Mobile Comput.*, pp. 1–1, 2021.

[37] Y. Wang, Q. Yao, J. T. Kwok, and L. M. Ni, "Generalizing from a few examples: A survey on few-shot learning," *ACM. Comput. Surv.*, vol. 53, no. 3, pp. 1–34, Jun. 2020.

[38] W.-Y. Chen, Y.-C. Liu, Z. Kira, Y.-C. F. Wang, and J.-B. Huang, "A closer look at few-shot classification," in *Proc. Int. Conf. Learn. Represent. (ICLR)*, New Orleans, Louisiana, USA, Sep. 2018.

[39] J. Snell, K. Swersky, and R. Zemel, "Prototypical networks for few-shot learning," in *Proc. Int. Conf. Neural Information Processing Systems. (NeurIPS)*, Red Hook, NY, USA, Dec. 2017, p. 4080–4090.

[40] F. Sung, Y. Yang, L. Zhang, T. Xiang, P. H. Torr, and T. M. Hospedales, "Learning to compare: Relation network for few-shot learning," in *Proc. IEEE Comput. Soc. Conf. Comput. Vis. Pattern Recognit. (CVPR)*, SLC,USA, Jun. 2018, pp. 1199–1208.

[41] K. Weiss, T. M. Khoshgoftaar, and D. Wang, "A survey of transfer learning," *J. Big. Data.*, vol. 3, no. 1, pp. 1–40, May 2016.

[42] J. Huang, B. Liu, C. Chen, H. Jin, Z. Liu, C. Zhang, and N. Yu, "Towards anti-interference human activity recognition based on wifi subcarrier correlation selection," *IEEE Trans. Veh. Technol.*, vol. 69, no. 6, pp. 6739–6754, 2020.

[43] D. Halperin, W. Hu, A. Sheth, and D. Wetherall, "Tool release: Gathering 802.11 n traces with channel state information," *ACM SIGCOMM comput. commun. review*, vol. 41, no. 1, pp. 53–53, 2011.